AD-A056 602 CAMBRIDGE UNIV (ENGLAND) DEPT OF ENGINEERING F/G 11/4
IMPROVING THE IMPACT AND FRACTURE RESISTANCE OF FIBROUS COMPOSI--ETC(U)
1977 P W BEAUMONT, J N KIRK, M MUNRO DA-ERO-75-G-009
UNCLASSIFIED CUED/C-MAT/TR.46-1977 NL

| OF |
AD
A056602

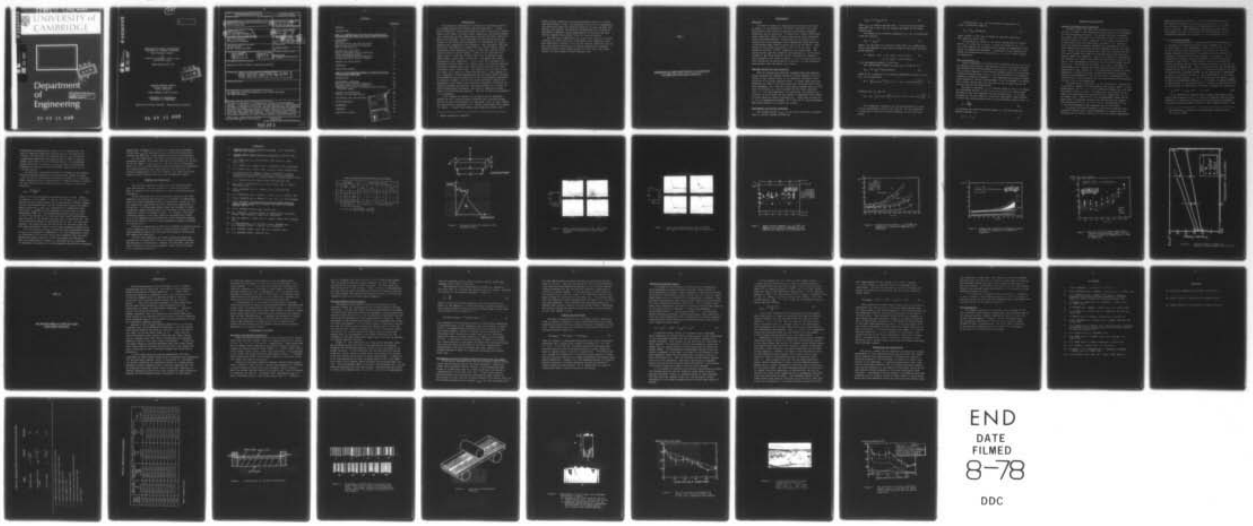

END
DATE
FILMED
8-78
DDC

LEVEL II (12 sc A016959

UNIVERSITY of CAMBRIDGE

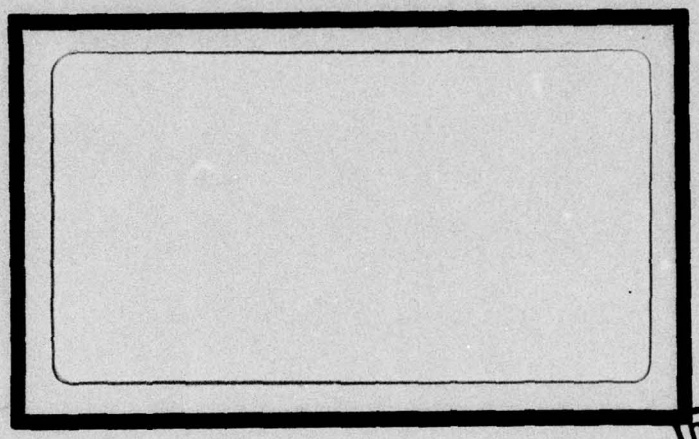

Department of Engineering

(12)

AD

IMPROVING THE IMPACT AND FRACTURE RESISTANCE OF FIBROUS COMPOSITES

Final Technical Report

by

Peter W.R. Beaumont, John N. Kirk
and Michael Munro

CUED/C-MAT/TR.46, 1977

EUROPEAN RESEARCH OFFICE,
United States Army,
London, England.

GRANT NUMBER DA-ERO-75-G-009

DEPARTMENT OF ENGINEERING,
UNIVERSITY OF CAMBRIDGE.

(1)

SECURITY CLASSIFICATION OF THIS PAGE *(When Data Entered)*

REPORT DOCUMENTATION PAGE

READ INSTRUCTIONS BEFORE COMPLETING FORM

1. REPORT NUMBER	2. GOVT ACCESSION NO. / 3. RECIPIENT'S CATALOG NUMBER
4. TITLE (and Subtitle): Improving the Impact and Fracture Resistance of Fibrous Composites.	5. TYPE OF REPORT & PERIOD COVERED: FINAL TECHNICAL REPORT, 1 Feb 75 - 31 Jan 78 / 6. PERFORMING ORG. REPORT NUMBER
7. AUTHOR(s): Peter W. R. Beaumont, John N. Kirk, Michael Munro	8. CONTRACT OR GRANT NUMBER(s): DAERO-75-G-009
9. PERFORMING ORGANIZATION NAME AND ADDRESS: Dept. of Engineering, University of Cambridge	10. PROGRAM ELEMENT, PROJECT, TASK AREA & WORK UNIT NUMBERS: 6.11.02A-1T161102B35E-00-489
11. CONTROLLING OFFICE NAME AND ADDRESS: USA R&S GP (EUR), Box 65, FPO New York 09510	12. REPORT DATE: 1977 / 13. NUMBER OF PAGES: 48
14. MONITORING AGENCY NAME & ADDRESS *(if different from Controlling Office)*	15. SECURITY CLASS. *(of this report)*: UNCLASSIFIED / 15a. DECLASSIFICATION/DOWNGRADING SCHEDULE

16. DISTRIBUTION STATEMENT *(of this Report)*

Approved for Public Release, Distribution Unlimited

17. DISTRIBUTION STATEMENT *(of the abstract entered in Block 20, if different from Report)*

CUED/C-MAT/TR.46-1977

18. SUPPLEMENTARY NOTES

19. KEY WORDS *(Continue on reverse side if necessary and identify by block number)*

(U) Composites: (U) Fibrous Composites: (U) Fracture Resistance: (U) Impact Resistance.

20. ABSTRACT *(Continue on reverse side if necessary and identify by block number)*

The report is the third in a trilogy on the fracture of fibrous composites prepared. It describes a study of the fracture mechanisms in fibrous composites. The report is divided into 2 sections; the first part describes the temperature and strain-rate effects on the crack initiation energy and crack initiation energy and crack propagation energy of a carbon fibre-epoxy resin composite and a glass fibre-epoxy resin composite. The second part describes a study of the fracture mechanisms in a hybrid fibrous composite containing carbon and glass fibres.

DD 1 JAN 73 1473 EDITION OF 1 NOV 65 IS OBSOLETE

UNCLASSIFIED

SECURITY CLASSIFICATION OF THIS PAGE *(When Data Entered)*

400 081

CONTENTS

INTRODUCTION

The potential advantages of combining two different fibres in a common matrix have already been demonstrated[1,2]. Novak and De Crescente[3] have investigated the impact behaviour of carbon fibre, glass fibre, and boron fibre composites, and hybrid composites containing various combinations of boron and glass fibres in epoxy resin systems. They concluded that the stress-strain behaviour of the fibre was instrumental in determining the impact strength and toughness of the composite. But even more, they proposed that the addition of glass fibre to carbon fibre or boron fibre/epoxy resin composites could, in some way, provide an unexpected bonus of impact energy. Chamis et al[4] used the Izod impact test to study the fracture behaviour of unidirectional carbon fibre, glass fibre, boron fibre, and Kevlar 49* aramid fibre/epoxy resin composites. It was found that different combinations of these fibres in a common epoxy resin matrix generally had impact energies which were significantly greater than those containing either fibre alone. The implications from both groups are clear; as a result of fibre hybridisation, there appears to be a synergistic effect demonstrated by the higher impact energies than predicted from the behaviour of the mono-filament composites. In contrast, however, the work of Hancox and Wells[5] showed this phenomenon to be absent; they predicted reasonably accurately the flexural strength and modulus, and impact energy of a variety of carbon fibre/glass fibre/epoxy resin hybrid composites simply using a rule-of-mixtures approach. The work of Harris and Bunsell[6] is in agreement.

In an attempt to clarify the situation and to determine whether or not a hybrid fibrous composite has a fracture energy above that which is predicted by a mixtures' rule, we have carried out some fracture experiments on a carbon fibre-epoxy resin composite (cfrp), a glass fibre-epoxy resin composite (gfrp), and a

---

* DuPont registered trademark.

hybrid fibrous composite containing different amounts of carbon and glass fibres. First, we evaluated the effects of temperature and strain-rate upon the fracture behaviour of cfrp and gfrp composites; and finally, we isolated the mechanisms of cracking in the hybrid composites using simple models of fracture and used them to explain the measured values of fracture energy.

The effects of temperature and strain-rate upon the fracture toughness of carbon and glass fibre-epoxy resin composites have been discussed in detail in two earlier reports "Improving the Impact and Fracture Resistance of Fibrous Composites", European Research Office, Grant Number DA-ERO-75-G-009, DDC AD AO 16959 August 1975 and DA-ERO-75-G-009 December 1976.

PART I

TEMPERATURE AND STRAIN-RATE EFFECTS ON THE FRACTURE OF CARBON AND GLASS FIBRE COMPOSITES.

EXPERIMENTAL

Materials

In order to assess the advantages of combining two kinds of fibre, it is necessary to have both individual composites fabricated so that relative strength and fracture toughness properties can be evaluated. To begin with, carbon fibre-epoxy resin composites (cfrp) and glass fibre-epoxy resin composites (gfrp) were manufactured. Preparation of the materials was essentially by hot-pressing of pre-impregnated fibre tape with a proprietary epoxy resin at about 130 ^{o}C and 300 kN/m^{2}. Post-curing of the plates took place at 150 ^{o}C for 16 hours. Four balanced cross-ply ($0^{o}/90^{o}$) composites were fabricated. The carbon fibres used were coded by the manufacturer, as HTS (high strength), HMS (high modulus) and AS (intermediate strength). Their properties are given in Table 1. All the fibres were surface treated by the manufacturer to provide a strong mechanical bond between fibre and epoxy resin matrix.

Specimen Design and Test Procedure

Work of fracture and fracture toughness data was obtained using prismatic bar samples loaded in 3-point bending, with the fibres in the surface layers of the composite oriented in the direction of principle applied stress. A single edge notch was machined into some of the test-pieces and the plane-strain fracture toughness, K_{IC}, critical strain energy release rate G_{IC}, and work of fracture, γ_F, were evaluated for the fibre composite (fig. 1). For some specimens, the compliance was measured as a function of notch depth and the change of compliance with change in notch depth was used to estimate G_{IC}. Tests were carried out in air at temperatures between -20 ^{o}C and 150 ^{o}C, using displacement-rates between 0.01 cm/min and 3 m/sec.

Measurement of Fracture Toughness

The maximum stress, σ_{max}, in the outer fibres of an elastic beam in 3-point bending is given by

$$\sigma_{max} = 1.5\ P_{max}\ L/b\ d^2 \qquad (1)$$

where P_{max} is maximum applied load, L is the distance between supports, and b and d are the breadth and depth of the beam, respectively.

The plane-strain fracture toughness, K_{IC}, can be calculated using the equation

$$K_{IC} = Y\ \sigma_{max}\ a^{\frac{1}{2}} \qquad (2)$$

where a is the depth of a surface crack and Y is a geometrical factor that depends on the size and shape of the crack and test-piece geometry[7]

$$Y = 6M/bd^2\ (1.93 - 3.07\ (a/d) + 14.53\ (a/d)^2 - 25.11\ (a/d)^3 + 25.8\ (a/d)^4) \qquad (3)$$

M is the bending moment of the beam.

The relationship between K_{IC} and G_{IC} is given by [8,9]

$$K_{IC} = (E^*\ G_{IC})^{\frac{1}{2}} \text{ approximately} \qquad (4)$$

where E* is a function of the elastic compliance values a_{11}, a_{22}, etc. of the composite;

$$E^* = \left\{(a_{22}a_{11}/2)^{\frac{1}{2}} \left[(a_{22}/a_{11})^{\frac{1}{2}} + (a_{66} + 2a_{12})/2a_{11}\right]^{\frac{1}{2}}\right\}^{-1} \qquad (5)$$

Combining eq. (4) and (5):

$$G_{IC} = K_{IC}^{\ 2} \left\{(a_{22}a_{11}/2)^{\frac{1}{2}} \left[(a_{22}/a_{11})^{\frac{1}{2}} + (a_{66} + 2a_{12})/2a_{11}\right]^{\frac{1}{2}}\right\} \qquad (6)$$

The "toughness" parameter G_{IC} can be calculated by inserting an experimental value of K_{IC} into eq. (6) and computing a value for E* from the elastic properties of the fibre and matrix.

Alternatively, G_{IC}, can be determined experimentally using a compliance analysis;

$$G_{IC} = P^2_{max} \, (dC/dA)/2b \qquad (7)$$

where (dC/dA) is the rate of change of specimen compliance with change in crack area.

The subscript $_I$ refers to the crack opening mode of failure and G_{IC} is called the *toughness*. Since the values of a_{11}, a_{22}, etc., are expected to be sensitive to changes in temperature, then E*will be temperature dependent. Evaluation of G_{IC} therefore requires the determination of K_{IC} and a_{11}, a_{22}, etc., over a range of temperature.

Work of Fracture, γ_F

Crack propagation in brittle fibre composites may be *controlled* by designing the flexural beam specimen in such a way that the maximum stored elastic strain energy in the beam at the onset of cracking is small compared to the fracture surface energy of the material. A square-sectioned beam (4 mm × 4 mm) was machined at its mid-point forming an isosceles triangle[10]. Each specimen was loaded in three-point bending at values of displacement rate ($\dot{y}$) between 1.25 mm/min and 3 m/sec, making sure that the apex of the triangle was on the tensile side of the bending beam.

The work of fracture, γ_F, is defined simply as the *total* energy, E_T, dissipated during *controlled* or *quasi-controlled* crack growth divided by twice the apparent fracture surface area. It is represented by the area under the load-time (deflexion) curve divided by twice the cross-sectional area of the triangular section (fig. 1):

$$\gamma_F = \left(\frac{E_T}{2bd}\right) \qquad (8)$$

γ_F includes the crack initiation energy, γ_i, and the crack propagation energy, γ_p:

$$\gamma_F = \gamma_i + \gamma_p \qquad (9)$$

RESULTS AND DISCUSSION

Carbon Fibre-Epoxy Resin Composites

Previous work[11] has shown the fracture stress and toughness of cfrp to depend on the properties of the fibre and the strength of the fibre-resin interface. The dynamic fracture toughness, K_{IC} values were calculated from load-time traces, and the shape of these curves is clearly dependent on the elastic properties of the carbon fibre and temperature (figures 2, 3). Figure 4 shows the fracture toughness parameter K_{IC} measured for cfrp at room temperature and plotted against specimen geometry and crack size. First, the high strength (HTS) cfrp has a greater failure load and a larger area under the load-time curve than the high modulus (HMS) cfrp composite. Second, an increase in temperature has resulted in a larger area under the non-linear portion of the curve. This represents an increase in the non-recoverable energy term in γ_F. No variation was found in K_{IC} over 5 decades of displacement rate; neither was there any significant effect of temperature on K_{IC} (figure 4). The differences between the three composites in terms of fracture stress and fracture toughness reflects the dependence of K_{IC} on the elastic properties of the carbon fibres. This accounts for the strain-rate and temperature *insensitivity* of the composites.

The total work of fracture, γ_F, as a function of temperature is plotted in figure 5 for quasi-static and dynamic tests. At low temperatures (-20 ^{o}C → r.t.), the difference between the slow bend and impact values is small; it becomes more significant as the temperature approaches the glass transition temperature (T_g) of the epoxy resin. Above 60 ^{o}C, the time-dependent nature of the epoxy resin is apparent, shown by the strain-rate and temperature sensitivity of γ_F i.e. at T > 60 ^{o}C, the position of the γ_F (T) curve depends on the response time of the matrix.

The crack initiation energies of the three cross-ply cfrp composites exhibit only a small dependence on temperature and increase only by about a factor of 2 over the entire temperature

range investigated (figure 6). In the low temperature region, the difference between γ_F and $G_{IC}/2$ is negligible ($2\gamma_F \sim G_{IC}$) but increase as T approaches T_g of the epoxy resin ($\sim$ 150 ^{o}C at $\dot{y}$ = 1 m/sec). This difference represented by the shaded area between the two solid curves for each composite, can be considered equivalent to the energy of crack propagation, γ_p.

Crack Propagation Energy

At low temperatures γ_F values measured in slow bending are in agreement with observed values of $G_{IC}/2$ (figure 6). It can be argued that in this temperature range (-20 ^{o}C to 50 ^{o}C), failure occurs by brittle fracture and the work of fracture simply evaluates the material's resistance to crack initiation in terms of stored elastic strain energy in the fibres. As the temperature increases, increasing amounts of fibrous fracture and matrix flow occurs. These modes of failure are energy absorbing processes and the crack propagation energy γ_p will become a function of temperature. This is represented by the shaded area between the solid γ_F (T) and $G_{IC}/2$ (T) curves in figure 6. The rate of increase of γ_p becomes greater as the temperature T approaches T_g and is *strain-rate dependent*. The contributions of the matrix fracture surface energy, γ_m, and the fibre pull-out energy, γ_{IIp}*, to the crack propagation energy, γ_p, is clearly a complex function of strain-rate, $\dot{\varepsilon}$, and temperature, T, as shown by the shift of the γ_F curve along the temperature axis with a change of $\dot{y}$ (figure 5):

$$\gamma_p\ (\dot{\varepsilon},T) = \gamma_{IIp}\ (\dot{\varepsilon},T) + \gamma_m\ (\dot{\varepsilon},T) \qquad (10)$$

It is difficult to separate the relative influences of the matrix and interface on γ_p, but a plot of observed fibre pull-out lengths as a function of temperature obtained from the scanning electron microscopy studies (figure 7) has a similar shape to the

---

* The subscript $_{II}$ refers to the shear mode of failure on a *microscopic* level.

γ_F (T) curve (figure 5). The values of mean fibre pull-out length should not be taken as absolute because of the few fracture surfaces studied in great detail.

It is interesting to note that changes in fibre pull-out lengths with variations in crack velocity (strain-rate), have been observed in unidirectional cfrp[12], gfrp[13] and carbon fibre-reinforced glass[14], which serves to illustrate the rate-dependence of γ_{IIp}.

Glass Fibre-Epoxy Resin Composites

An increase in strain-rate of the order of one-thousand times has resulted in a significant increase in the value of the fracture energy parameters γ_F and G_{IC}, where G_{IC} has been calculated by inserting experimental values of K_{IC} into eq. (6) and using a value of E* of 14.1 GN/m^2 (fig. 8).

Values of γ_F and $K_{IC}^2/2E^*$ are similar at room temperature and are greater than values of $G_{IC}/2$ obtained using a compliance analysis; the latter term, however, is less dependent on strain-rate.

It is interesting to note that the strain-rate dependence of γ_F and G_{IC} at room temperature is less pronounced at 100 ^oC (fig. 9). For a given strain-rate, γ_F and G_{IC} are independent of temperature up to 110 ^oC; at T > 110 ^oC, the work of fracture, γ_F, increases dramatically whilst G_{IC} decreases (fig. 10).

Interpretation of Fracture Energy

Crack initiation occurs by the breakage of fibres at flaws along the length of the fibre and cracking in the matrix; these microcracking processes take place in a fracture process zone close to the crack tip in the composite material. The process of crack growth involves separation of 2 fracture surfaces at the crack tip which can result in pulling out of broken fibres from the matrix. Assuming that reloading of the fibre occurs after fibre fracture, then the maximum length of protruding fibre out of the surface of the cracked matrix will be $\ell_c/2$ where ℓ_c is defined by [15]

$$\ell_c = \sigma_f \, d/2 \, \tau_i \qquad (11)$$

ℓ_c is called the critical fibre length, σ_f is the fibre strength, d is fibre diameter and τ_i is the interfacial shear stress.

The extension of a crack in a fibre composite may be considered a two stage process: (1) crack initiation and (2) crack propagation. If the length of fibre pulled out of the resin matrix is small compared to the size of the fracture process zone, then the work done in separating the crack surfaces at the tip will include the work to pull the fibres out of their sockets, γ_{IIp}. Conversely, if the fibre pull-out length is similar or larger than the fracture process zone, then the crack initiation energy, γ_i may simply be equated to

$$G_{IC} \simeq 2\gamma_i = \gamma_f + \gamma_m + \gamma_d \qquad (12)$$

where γ_f and γ_m are the fracture surface energies of the fibre and the matrix, respectively, and γ_d is the energy lost when a loaded fibre debonds and snaps.

When a fibre close to the crack tip snaps, the amount of energy released is [16]

$$\Delta E = \pi d^2 \, \sigma_f^2 \, \ell_c/12 \, E_f \qquad (13)$$

where E_f is the fibre modulus and ℓ_c corresponds to the length of fibre over which load relaxation has occurred. For a fibre composite having a fibre volume fraction V_f

$$\gamma_d = 2 \, \Delta E V_f/\pi d^2 = V_f \, \sigma_f^2 \, \ell_c/ 6E_f \qquad (14)$$

and γ_d is the "fibre debonding energy" per unit area of fracture surface.

The maximum length of protruding glass fibre out of the epoxy resin is about 10^{-3} m. Inserting the values of $V_f = 0.32$, $\sigma_f = 2.10$ GN/m^2, $E_f = 72$ GN/m^2 and $\ell_c = 4 \times 10^{-3}$ m into eq. (14) gives 13 kJ/m^2. This value is in remarkable agreement with the

experimental measurements of $G_{IC}/2$ ($\dot{y}$ = 0.1 cm/min)(fig. 8) using a compliance analysis and this must be considered fortuitous. The critical strain energy release G_{IC} obtained in a compliance experiment does not include the work to extract broken glass fibres out of a cracked matrix. The difference between the work of fracture γ_F and $G_{IC}/2$ may be considered therefore as the work to pull the broken glass fibres out of a cracked matrix.

An analysis[17] originally derived to account for the energy dissipated during extraction of discontinuous fibres of length ℓ_c may be used to approximate the pull-out energy of a continuous fibre composite having a distribution of fibre strengths by assuming that the mean fibre pull-out length is equal to $\ell_c/4$, and therefore

$$\gamma_{IIp} = \frac{V_f \tau_i' \ell_c^2}{12d} \qquad (15)$$

where τ_i' is the "frictional" interfacial shear stress. Using a value of τ_i' = 0.5 MN/m^2 [18] and d = 10^{-5}m then γ_{IIp} = 5.4 kJ/m^2. The work to pull glass fibres out of the matrix is 5 kJ/m^2 approximately, which agrees well with the difference between the experimental values of γ_F and $G_{IC}/2$ (obtained in a compliance test). This term, γ_{IIp} appears to be dependent on strain-rate at room temperature (fig. 8). The difference between γ_F and $K_{IC}^2/2E^*$ at 100 ^oC may be due to the fibre pull-out length being greater than the size of the fracture process zone at the crack tip. The crack initiation energy is then given by eq. (12). As the crack extends, the broken fibres are pulled out of the matrix and the work done contributes mainly to the crack propagation energy term.

Fig. 10 shows γ_F and G_{IC} (calculated from experimental values of K_{IC}) as a function of temperature. At room temperature, these two parameters have similar values which suggests that the crack propagation energy and crack initiation energy are identical. When the temperature is raised, γ_F increases and G_{IC} decreases. It indicates an increase in crack propagation energy with increasing

temperature, probably as a result of a temperature dependence of the term γ_{IIp}. The decrease in G_{IC} at elevated temperatures reflects the decrease in the fracture stress of the composite.

At room temperature, the crack initiation energy and crack propagation energy are similar and consist principally of the sum of the two terms, γ_d and γ_{IIp} ($\gamma_m \sim 300$ J/m^2 and is negligible), where $\gamma_d \sim 2\text{-}3\ \gamma_{IIp}$. This energy is dissipated during the formation of a microfracture process zone ahead of the crack tip. At elevated temperatures ($\sim 120\ ^{o}$C), however, the crack initiation energy is about one-third of the crack propagation energy.

SUMMARY AND CONCLUSIONS

The fracture behaviour of cfrp and gfrp composites have been investigated. We have attempted to separate the total work of fracture into the energies of crack initiation and crack propagation.

It was found that the crack initiation energy of the cfrp composite was essentially insensitive to changes in temperature, while the crack propagation energy increased by a factor of 3 as the temperature approached the glass transition temperature of the matrix. A fractography study showed the increase in crack propagation energy corresponded to an increase in fibre pull-out length by a factor of between 2 and 3. In contrast, the crack initiation energy of the gfrp composite decreased by a factor of 2 as the temperature approached the glass transition temperature of the matrix, while the crack propagation energy increased by a factor of 2.

This may be explained in terms of a decrease in fracture stress of the composite and an increase in fibre pull-out energy. The fibre debonding energy and fibre pull-out energy is strain-rate and temperature sensitive.

For the cfrp composite, the crack initiation energy was insensitive to strain-rate, while the crack propagation energy was sensitive to strain-rate. However, for the gfrp, both the crack initiation and crack propagation energy terms increased with increasing strain-rate.

REFERENCES

1. Composite Materials: Testing and Design (2nd Conference), ASTM STP 497, (1972).

2. Foreign Object Impact Damage to Composites, ASTM STP 568, (1974).

3. R.C. NOVAK and M.A. DE CRESCENTE, ASTM STP 497, (1972) pp311-323.

4. C.C. CHAMIS, M.P. HANSON and T.T. SERAFINI, ibid, pp324-349.

5. N.L. HANCOX and H. WELLS, AERE (Harwell) Report AERE-R.7016.

6. B. HARRIS and A.R. BUNSELL, "Impact properties of glass fibre-carbon fibre hybrid composites", School of Applied Sciences, University of Sussex, Brighton, England (April 1975).

7. J.E. SRAWLEY and W.F. BROWN (1964) ASTM STP 410, p13.

8. G.C. SIH, P.C. PARIS and G.R. IRWIN (1965), Int. J. Fract. Mechanics 1 189.

9. P.W.R. BEAUMONT and W.L. SERVER (1975), ASTM STP 580 443-457.

10. H.G. TATTERSALL and G. TAPPIN, J. Mat. Sci., 1, (1966), 296.

11. P.W.R. BEAUMONT and B. HARRIS, J. Mat. Sci., 7, (1972),p1265.

12. P.W.R. BEAUMONT, Fracture and fatigue of carbon fibre reinforced epoxy resin, Ph.D. thesis, University of Sussex, England (1971).

13. R.G.C. ARRIDGE, Nature, 223, (1969), 941.

14. D.C. PHILLIPS, "Fracture energy of carbon fibre reinforced glass", AERE (Harwell), Report No. AERE-R6916.

15. See for example A. KELLY and G.T. DAVIES (1965), Met. Reviews 10 1.

16. J. FITZ-RANDOLPH, D.C. PHILLIPS, P.W.R. BEAUMONT and A.S. TETELMAN (1972), J. Mater. Sci. 7 289-294.

17. A.H. COTTRELL (1964), Proc. Roy. Soc. Series A 282.

18. L.J. BROUTMAN (1968), ASTM STP 452.

TABLE I. Elastic Properties of Carbon Fibres and $0^{\circ}/90^{\circ}$ CFRP ($V_f = 0.60$) Composites.

FIBRE PROPERTIES			ELASTIC CONSTANTS OF $0^{\circ}/90^{\circ}$ CFRP							
TYPE	STRENGTH (GNm^{-2})	MODULUS (GNm^{-2})	E_{11} (E_{22}) (GNm^{-2})		G_{12} (GNm^{-2})		ν_{12} (ν_{21})		E* (Plane stress) (GNm^{-2})	
			$20^{\circ}C$	$175^{\circ}C$	$20^{\circ}C$	$175^{\circ}C$	$20^{\circ}C$	$175^{\circ}C$	$20^{\circ}C$	$175^{\circ}C$
HMS	2.06 - 2.2 (2.07)*	365 - 405 (379)	89.5	89.5	4.47	3.44	0.05	0.02	38	34
HTS	2.68 - 3.16 (276)	248 - 290 (262)	79	67.5	4.46	1.25	0.05	0.02	35	18
AS	2.42 - 2.54 (248)	183 - 234 (186)	63.2	58.5	4.12	2.06	0.05	0.02	30	21

HMS - high modulus fibres HTS - high strength fibres AS - intermediate strength fibres

* Figures in brackets are mean values

E* - "Effective Modulus" $\left\{ \left(\frac{a_{11}a_{22}}{2} \right)^{\frac{1}{2}} \left[\left(\frac{a_{22}}{a_{11}} \right)^{\frac{1}{2}} + \frac{a_{66} + 2a_{12}}{2a_{11}} \right]^{\frac{1}{2}} \right\}^{-1}$

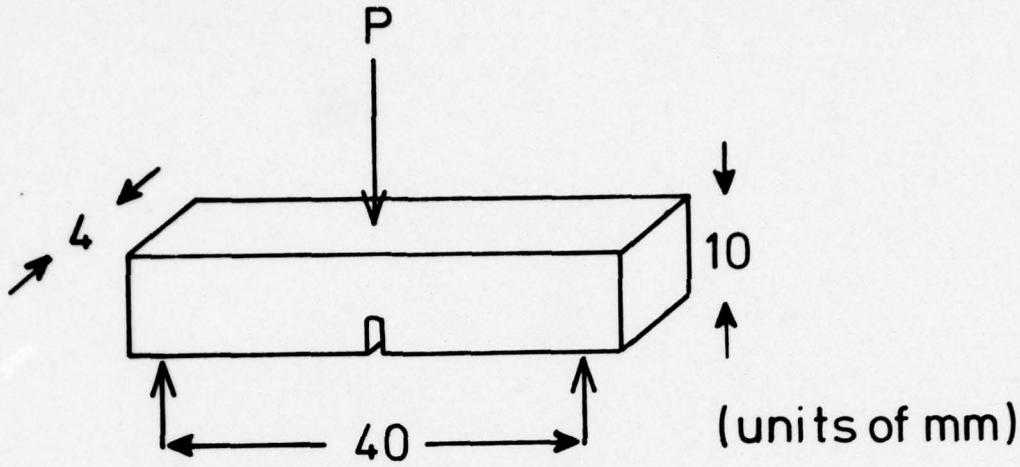

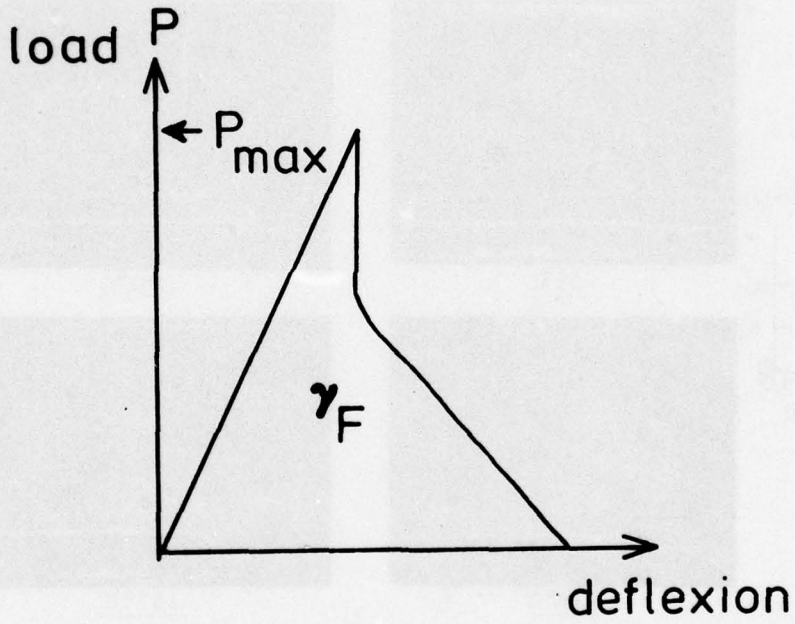

Figure 1 Specimen design and typical load/ deflexion curve.

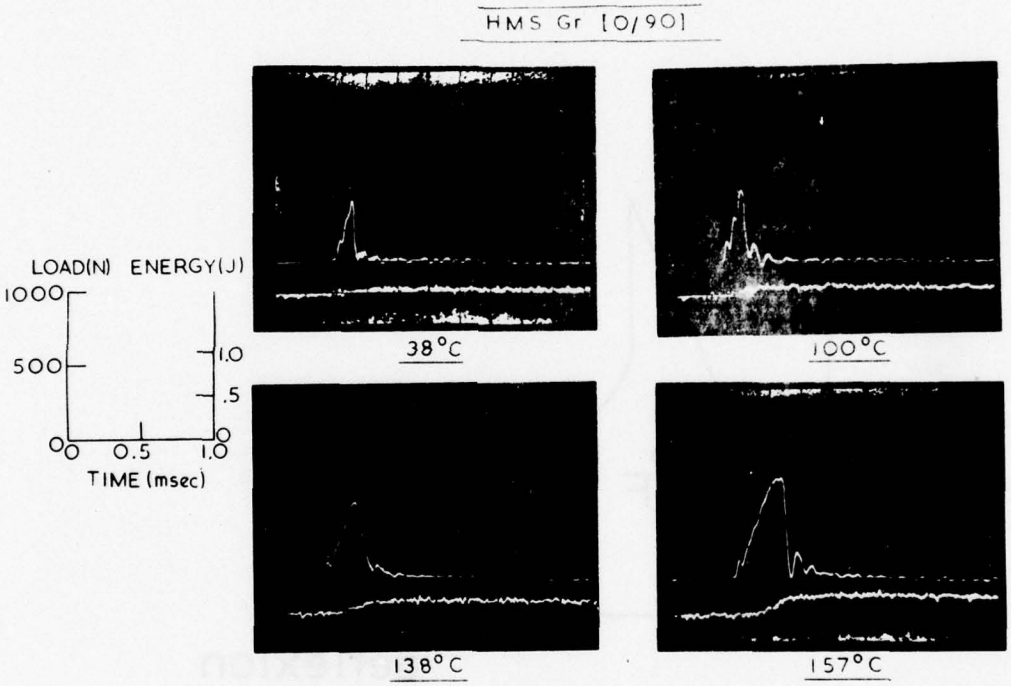

Figure 2 Typical load/energy/time traces for a HMS $0^{o}/90^{o}$ cfrp composite obtained over a range of temperatures.

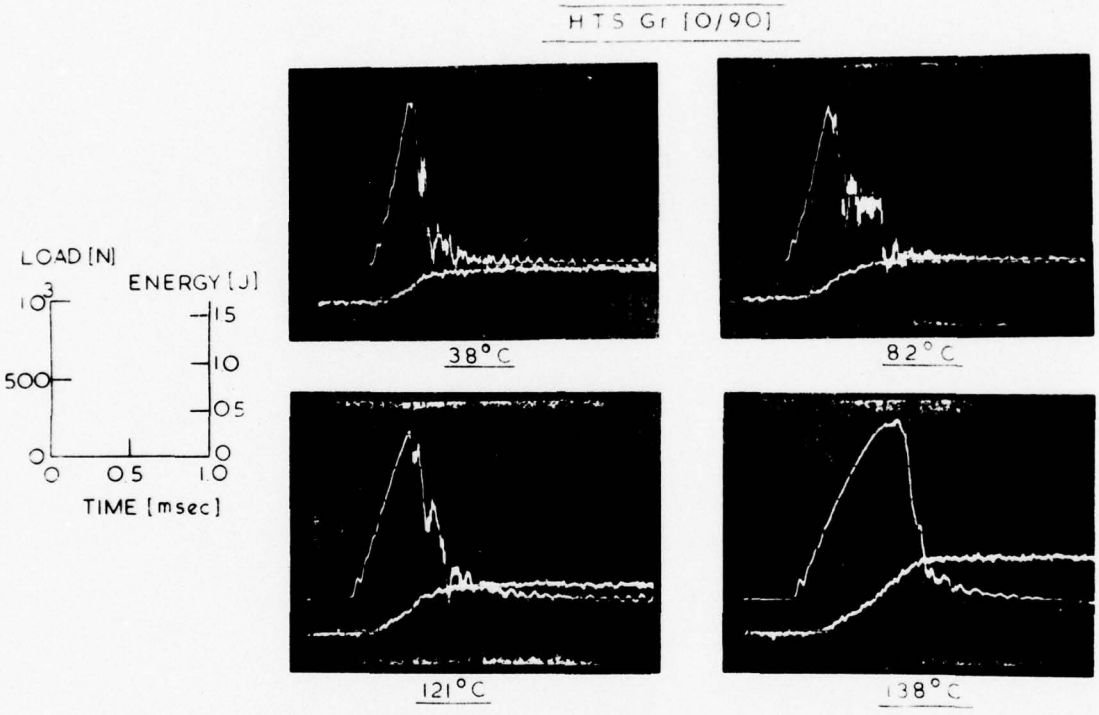

Figure 3 Typical load/energy/time traces for a HTS $0^{o}/90^{o}$ cfrp composite obtained over a range of temperatures.

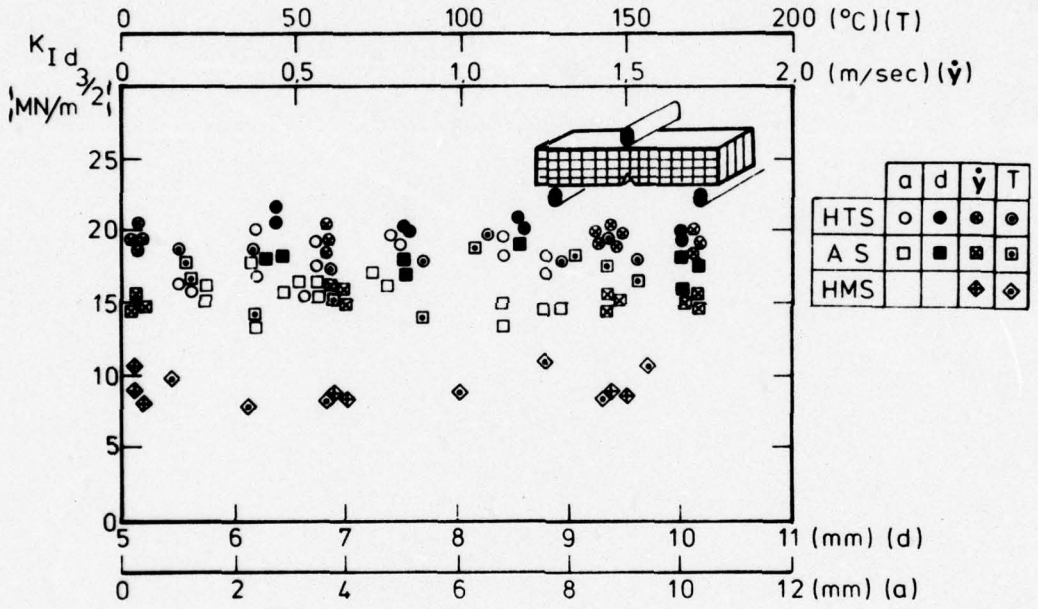

Figure 4 Dynamic fracture toughness, K_{Id}, of $0^o/90^o$ cfrp composites as a function of specimen and crack geometry, and temperature and displacement-rate.

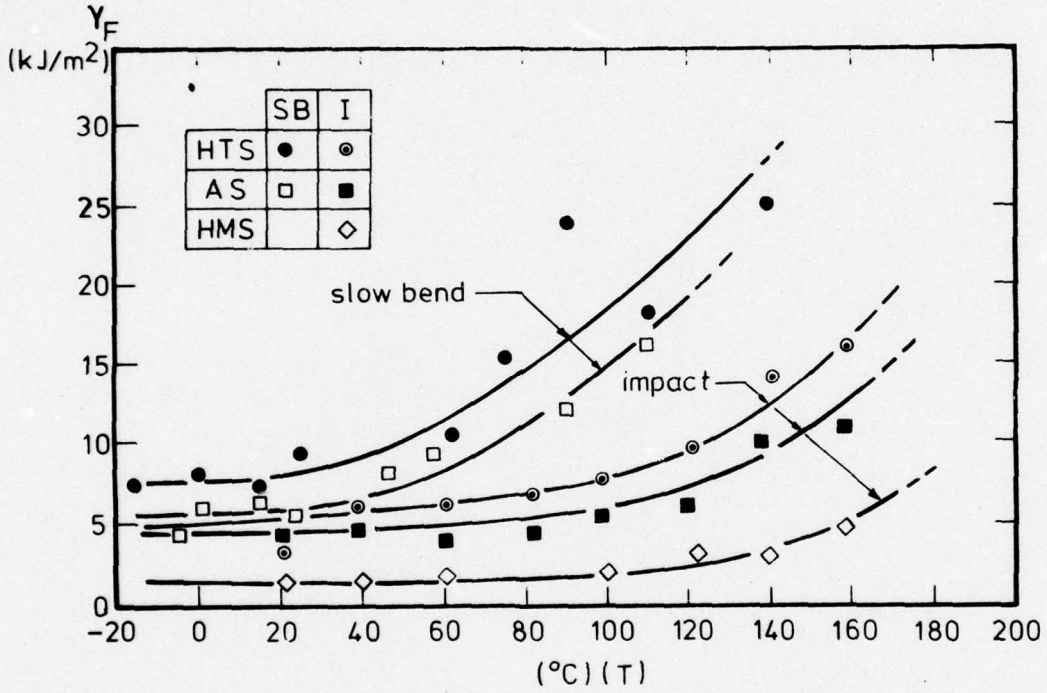

Figure 5 The total work of fracture, γ_F, of $0^o/90^o$ cfrp composites as a function of temperature and strain-rate.

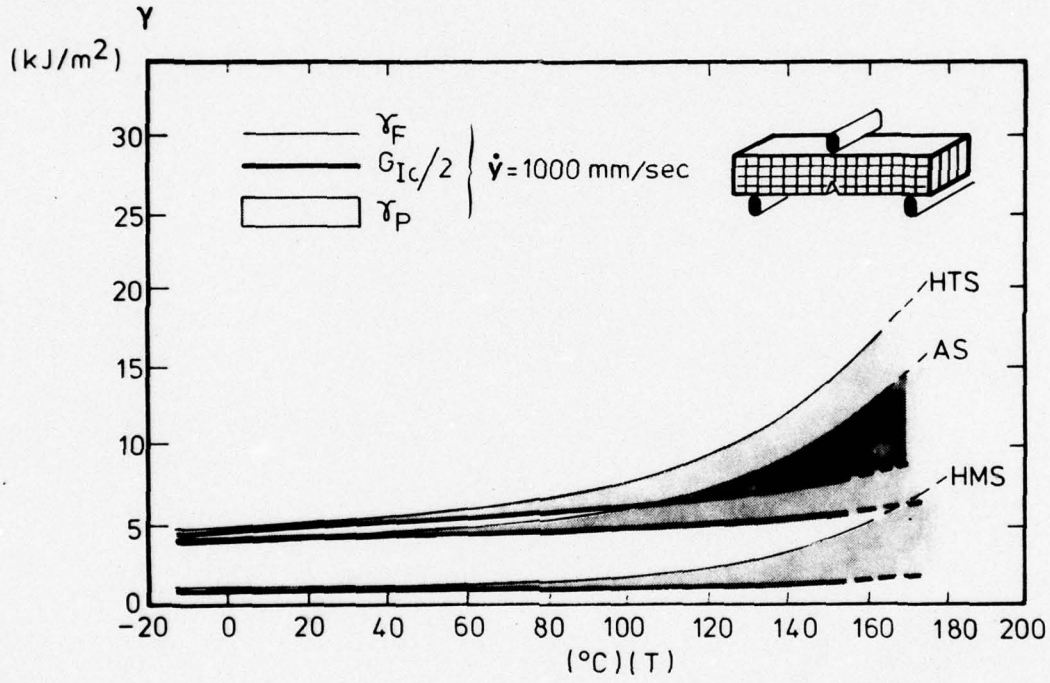

Figure 6 Dynamic crack initiation and propagation energies of $0^{o}/90^{o}$ cfrp composites as a function of temperature.

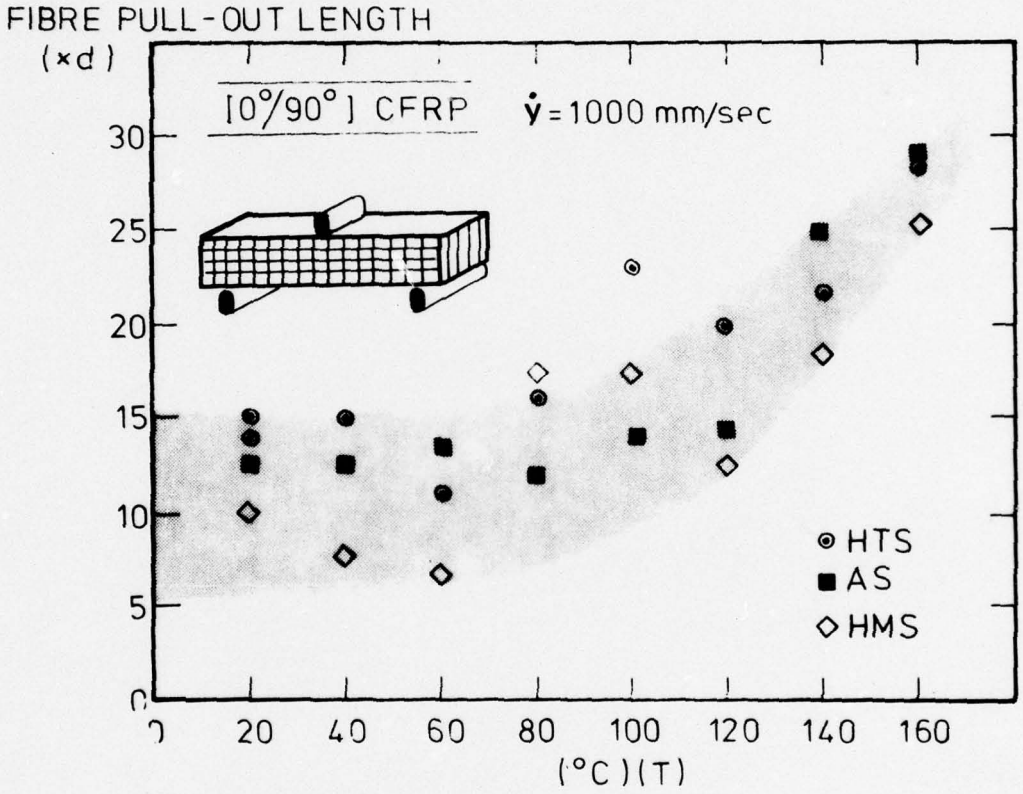

Figure 7 Mean fibre pull-out lengths obtained from a scanning electron microscope study of fracture surfaces of $0^{o}/90^{o}$ cfrp composites over a range of temperatures.

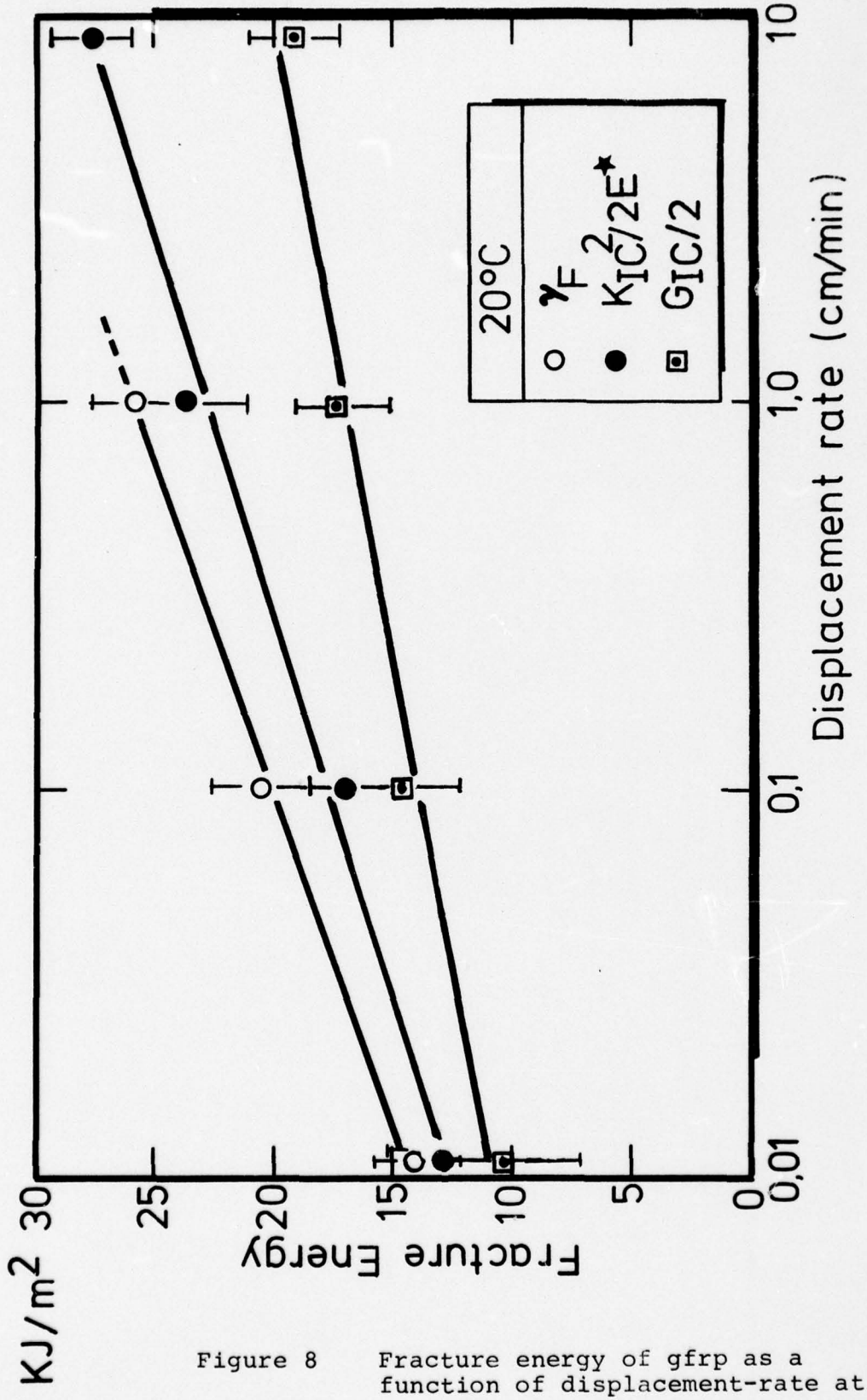

Figure 8 Fracture energy of gfrp as a function of displacement-rate at 20 °C.

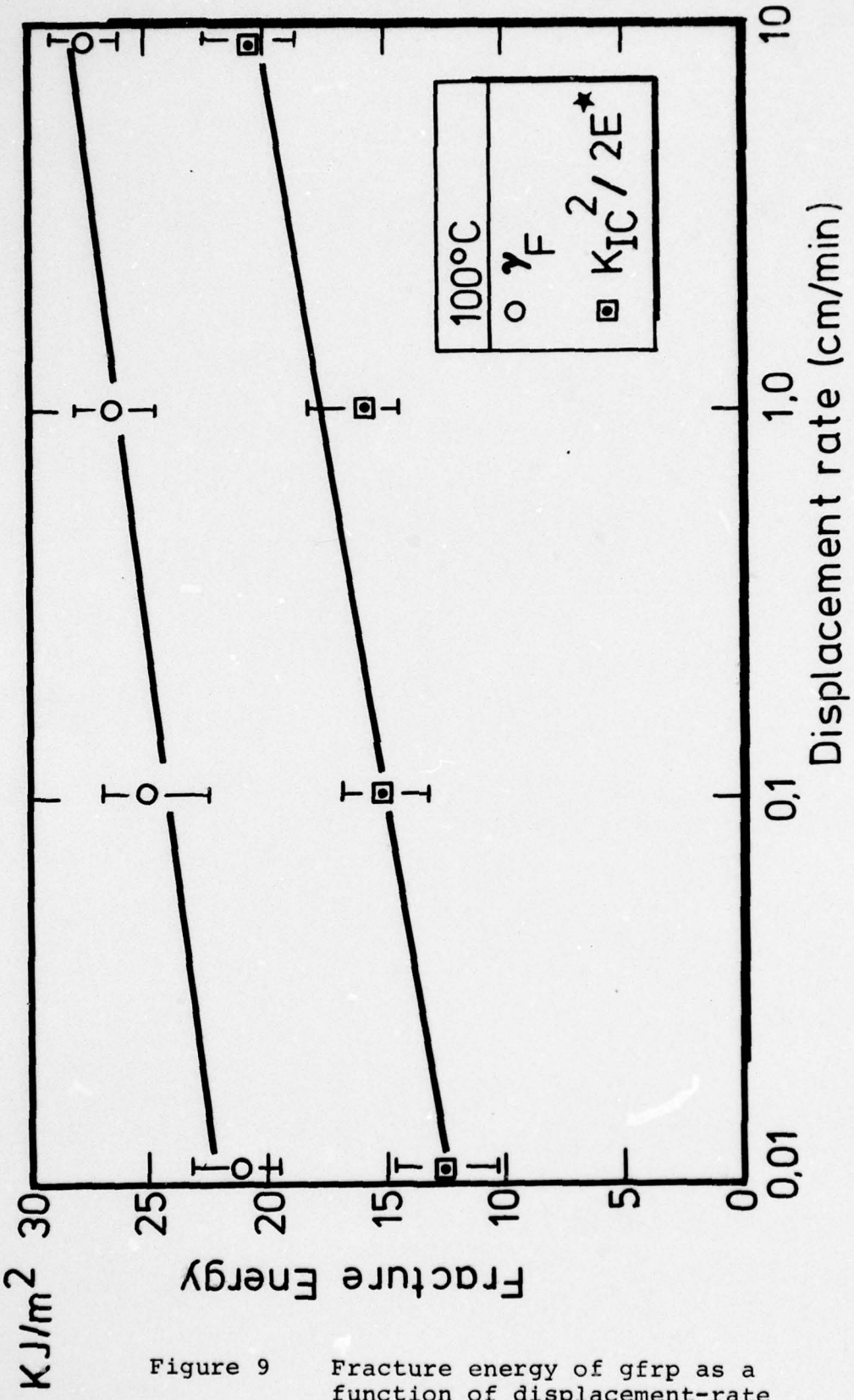

Figure 9 Fracture energy of gfrp as a function of displacement-rate at 100 °C.

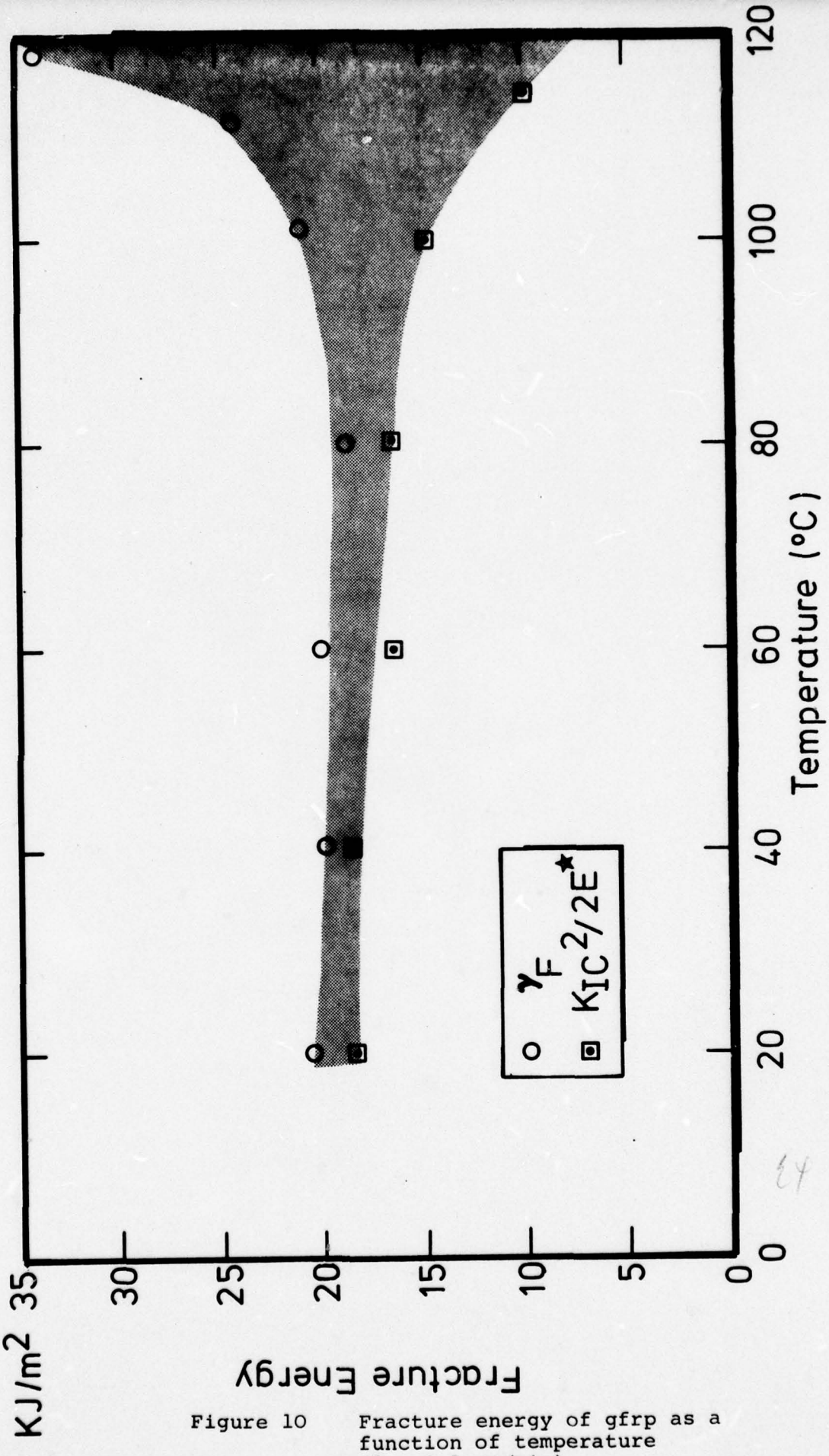

Figure 10 Fracture energy of gfrp as a function of temperature ($\dot{y}$ = 0.1 cm/min).

PART II

THE FRACTURE ENERGY OF CARBON AND GLASS FIBRE HYBRID COMPOSITES

INTRODUCTION

Fracture mechanisms at the microscopic level, in fibre strengthened brittle materials, can combine to give different kinds of macroscopic fracture behaviour [1]. Carbon fibre reinforced epoxy resin composites (cfrp), for instance, have a fracture toughness which is derived primarily from the frictional work to extract broken fibres out of a cracked matrix [2], while the fracture toughness of glass fibre reinforced epoxy resin composites (gfrp)originates from the dissipation of energy in fibre-matrix debonding [3] and post-debond fibre sliding processes [4,5]. It is logical to assume, therefore, that the combination of carbon fibres and glass fibres in the same matrix will produce a fibrous composite which possesses some of the microfracture characteristics of the two individual composite systems.

Whether or not a hybrid fibrous composite has a fracture toughness that can be predicted by assuming a rule of mixtures relationship between the works of fracture of cfrp and gfrp is not clear; on the one hand, Chamis et al [6] imply that for carbon fibre/glass fibre hybrid composites the impact energy may be increased above that which is predicted by a mixtures' equation, while on the other, Harris and Bunsell [7] found that the impact energy of notched specimens made from carbon fibre/glass fibre hybrids followed the mixture rule, even though the work of fracture of their unnotched samples fell below such a prediction.

In this study detailed fracture experiments have been undertaken on model carbon fibre/glass fibre/epoxy resin composites for two principal reasons; first, to establish in a systematic way whether combining two dissimilar fibres in a common matrix produces a hybrid composite with a fracture toughness that can be predicted accurately using a rule of mixtures' equation, or whether synergistic effects can occur because of some interaction between the two different fibres; and second, to see whether

the fracture energy of such hybrids can be estimated using existing fracture models for brittle fibrous composites. Previous studies [7 - 12] have made this comparison difficult for three main reasons: (1) there was a large amount of scatter in the experimental data due to differences in microstructure from specimen to specimen: (2) only a small number of different fibre combinations was examined and (3) the fibre-matrix debonded and fibre pull-out lengths could not be precisely measured.

In the present work, an attempt has been made to overcome these difficulties by fabricating reproducible model specimens from single layer, uni-directional fibre hybrid tapes. A total of ten carbon fibre/glass fibre ratios were used and the choice of a transparent epoxy resin matrix permitted easy recognition and measurement of fibre debonded zones. A specimen was designed to ensure that all of the fibres failed in tension (rather than in both tension and compression as generally occurs in 3-point bend tests) and that fibre pull-out lengths could be more accurately measured than in earlier studies.

EXPERIMENTAL PROCEDURE

Materials and Specimen Preparation

Tapes have been produced which contain unidirectional E-glass fibre tows and high strength (type II) carbon fibre tows in ratios of 1:0, 4:1, 3:1, 1:1, 1:4 and 0:1, respectively. These tapes were used to prepare model composites containing different ratios (by volume) of carbon fibres to glass fibres, i.e. 0/100, 13/87, 23/77, 37/63, 44/56, 54/46, 64/36, 70/30, 83/17 and 100/0. The properties of the carbon and glass fibres are presented in Table I. An epoxy resin (Ciba-Geigy CY219) with hardener (HY219) in the ratio of 2:1 (by volume) was used as the matrix.

Casting of the model composite systems involved three stages: first, a piece of tape (150 mm × 150 mm) was immersed in a solution of equal volumes of epoxy resin plus hardener, and of acetone. Next, the wetted tape was heated in an oven to 80 ^{o}C for 15 minutes to evaporate the acetone. The epoxy resin impregnated tape was gently stretched across a split-frame mould (Fig. 1). Finally, a

mixture of epoxy resin and hardener at 100 °C was slowly poured into the mould at one end, passing beneath the tape, and displacing air as it slowly filled the mould. The cast plate was then cured at 60 °C for 24 hours. This technique of impregnating the tape with an epoxy resin/acetone solution followed by casting hot resin around the tape ensured excellent wetting of fibres and reproducibility of each model hybrid composite.

Specimen Design and Test Methods

Rectangular beams tested in three point bending was the procedure chosen for investigating the fracture energy of hybrid composites. The specimen width varied as determined by the number of carbon fibre and glass fibre tows necessary to give a particular carbon-to-glass fibre ratio. The arrangement of the fibre tows for each group of specimens is shown schematically in Figure 2. The thickness of the specimen was determined by considering the following three requirements: (1) the single layer of tape had to be offset from the central plane towards the tensile face so that when each specimen was loaded in flexure all of the fibres were loaded in tension; (2) it was necessary to make a saw cut across the tensile face of the specimen to aid crack initiation; (3) the thickness of the pure epoxy resin layer must be as thin as possible to minimise unstable fracture.

Cooper [13], has shown that in a three point bend test width and thickness fixed, the span of the specimen is an important parameter for determining whether failure occurs by stable or unstable cracking. It was found here for the most brittle fibrous composite, carbon fibres in epoxy resin, that spans of 20 mm and 40 mm gave stable and unstable fracture respectively. A length of 20 mm (corresponding to a span to depth ratio of 10:1) was therefore chosen which ensured stable fracture and prevented shear failure. Thus rectangular beams 30 mm long, 2.25 mm thick and 6 to 9 mm wide were machined from the cast plates. Each specimen was tested in three point bending (Fig. 3) at 18 °C (±2 °C) at a displacement

rate of 2 mm/minute on an Instron testing machine (model TTC) equipped with a 5000 N load cell.

The integral of the load-deflection curve was equated to the total work (U) to break the specimen into two pieces. The work of fracture of the fibrous composite is given by

$$\gamma_F = \frac{E_T}{2A} \tag{1}$$

where A is the total cross sectional area of the ends of the fibres in the composite. "Volume fraction" therefore refers to the relative amount of carbon fibres or glass fibres in the total fibre content of the composite, i.e.

$$V_{f(\text{carbon fibre})} + V_{f(\text{glass fibre})} = 1 \tag{2}$$

Any discussion of the fracture energy of these hybrid composites is therefore based on the assumption that the material is essentially a two-phase system where the matrix only serves to bind the fibres together. Work of fracture values calculated in this manner will therefore be higher than those of structural composites where the volume fraction of fibres is of the order of 0.60. A variation in both the volume of fibres in a carbon and a glass tow and in the number of carbon fibre and glass fibre tows from one group of specimens to the next, necessitated a normalising of the work of fracture data with respect to a standard volume of fibre in a specimen containing five carbon fibre tows.

Measurement of Fibre De-Bonded Length and Fibre Pull-Out Length

Fibre-matrix debonded zones and the protruding ends of broken fibres can be clearly seen in the model specimens. Pulled out fibres were distinctly visible against a light background when viewed in transmitted light on a Zeiss projection microscope at a magnification of 50 times (Fig. 4b). A tracing was made of each protruding tow by carefully following the dark outline of the pulled out fibre and the fracture surface of the matrix (Fig. 4a). The maximum average pull-out length, $\bar{\ell}_{max}$, for each protruding tow

was then determined by dividing the area of the tracing by the width of the tow. When the microscope was used in the reflected light mode the fibre debonded zones were clearly visible against a dark background and the average fibre debonded length was obtained in a similar manner. It was verified, by observation of the opposite face, that the extent of the debonded zones was constant through the thickness of each fibre tow. The maximum fibre pull-out length and fibre debonded length of each tow in all specimens were measured. Final average fibre debonded lengths and maximum fibre pull-out lengths for each group of model composites was found by adding the average values for each tow and dividing by the total number of tows.

RESULTS AND DISCUSSION

The work of fracture data for the hybrid fibrous composites shown in Figure 5 exhibits a linear relationship with the volume fraction of carbon fibres for volume fractions of between 0.37 and 0.64. These values are still less than predicted by the rule of mixtures equation (Table II);

$$(\gamma_F)_{HYBRID} = (V_f\gamma_F)_{cfrp} + (V_f\gamma_F)_{gfrp} \qquad (3)$$

There is, however, a pronounced departure from a rule of mixtures prediction for a carbon fibre content of between 13 - 37 % and 70 - 90 %. A 25 % and 40 % decrease between the predicted and measured values of work of fracture exists at carbon fibre contents of approximately 23 and 83 % respectively. Cohibition and not a synergisitc improvement in fracture energy appears to determine the fracture behaviour of carbon fibre/glass fibre/epoxy resin hybrid composites. Figure 6 is a SEM photomicrograph of a typical fracture surface of a hybrid composite showing the pulled-out carbon fibres and glass fibres. It is viewed from the point of loading and shows a tensile failure of the fibres.

Analysis of Fracture Energy

In a model of the fracture of brittle fibrous composites, crack propagation occurs by matrix cracking, shear failure at the fibre-matrix interface, fibres snapping at weak points, fibres retracting in their matrix sockets and by the extraction of broken fibre ends as the two surfaces of a cracked matrix separate. Such fracture processes have been analysed and simple equations derived for their associated energies (Table 111). If for carbon fibre/epoxy resin composites, the work of fracture is controlled primarily by the fibre pull-out mechanism [2], while fibre debonding [3,4], post-debond sliding [4] and fibre pull-out [4,5] are the major energy absorbing processes in glass fibre/epoxy resin composites, then the total theoretical work of fracture of a fibrous composite containing both carbon fibres and glass fibres may be the sum of these separate energy terms:

$$\gamma_T = (\gamma_p)^c + (\gamma_d)^g + (\gamma_{pdf})^g + (\gamma_p)^g \qquad (4)$$

In physical terms, energy is dissipated when a debonded fibre snaps and its stored elastic strain energy is not transferred to the surrounding material but lost as kinetic, acoustic and thermal energies. This results in the retraction of fibre ends in their sockets. An increase in load on the composite causes the broken fibre to slide relative to the matrix over its entire debonded length. The differential displacement between fibre and matrix is assumed in the model to be equal to the product of the fibre debonded length and the difference in failure strains of fibre and matrix, $y\Delta\varepsilon$. Work is done when sliding occurs against friction at the interface. Additional energy may be expended during the extraction of broken fibre ends against a restraining "frictional" shear force when the matrix crack extends.

It is possible to estimate the relative contributions of these four energy terms for the two fibres by using known values of material constants (Table I), measured values of fibre debonded and fibre pull-out lengths (Table II), and by making certain assumptions of the other parameters which we have been unable to measure.

It was assumed that the fibre pull-out length varies linearly through the thickness of each tow between zero and the maximum fibre pull-out length. The average fibre pull-out length, $\bar{\ell}$, is therefore equal to $\frac{\ell_{max}}{2}$ and it is these values which are used in the appropriate energy terms. In the pull-out equation, (Table III), the average pull-out length is assumed to be $\bar{\ell} = \frac{\ell_c}{4}$ [14], where ℓ_c is the critical fibre length. Using the relationship $\frac{\tau}{d} = \frac{\sigma_f}{2\ell_c}$ [15] and $\bar{\ell} = \frac{\ell_c}{4}$, the post-debond friction energy equation becomes

$$\gamma_{pdf} = \frac{V_f \sigma_f y^2 \Delta\varepsilon}{8\bar{\ell}} \qquad (5)$$

It was also assumed that the differential strain between fibre and matrix, $\Delta\varepsilon$, used in connection with the post-debond friction energy term, has extreme values of 0.001 and 0.024, (Table I). If $\Delta\varepsilon = 0.010$, then the shape of the theoretical work of fracture curve, γ_T, matches that of the experimental curve remarkably well but the model consistently overestimates the experimental measurements, (Fig. 7). This is not unexpected since the calculated value for each energy term that appears in the fracture energy equation (4) is an upper bound.

Examination of the four theoretical energy curves (standard deviations given in Table IV), shows that the debonding energy of the glass fibres and the work to extract broken carbon fibres and glass fibres from the matrix follows a linear relationship with fibre volume fraction, as would be expected from the form of each equation. However, the shape of the theoretical curve for post-debond friction energy is not linear, but is very similar to that of the theoretical work of fracture curve, (Fig. 7). These results show that for the model glass-rich hybrid fibrous composites at least, the post-debond friction energy term is a major component of the total work of fracture. For the glass fibres, the fibre debonding energy and fibre pull-out energy terms are comparable in magnitude and the work of fracture of carbon fibre composites can be adequately explained using the fibre pull-out model. The debonded lengths of the carbon fibres were measured and found to be typically less than 1 mm which corresponds to a maximum debonding energy of 6 kJm^{-2}

and a post-debond friction energy of 4.8 kJm^{-2} assuming $\Delta\varepsilon = 0.014$ (Table I), and were thus not considered to be significant. The work of fracture of the hybrid fibrous composite can therefore be equated to the sum of the following energy terms:

$$(\gamma_F)_{HYBRID} = (\gamma_p)^c + (\gamma_d)^g + (\gamma_{pdf})^g + (\gamma_p)^g \qquad (6)$$

Some interaction between carbon fibres and glass fibres is responsible for the variation in the post-debond energy term for glass fibres in the hybrid composite. This term accounts for the unexpected shape of the glass-rich portion of the work of fracture curve. Fibre debonded length is the key parameter in this energy term and the general shape of the work of fracture curve is determined, therefore, by the effect of carbon fibres on the glass fibre debonding process. It requires only a 20 % (by volume) replacement of glass fibres by carbon fibres for a drop of about 25 % in fracture energy with respect to a rule of mixtures prediction. It is of interest to note that at the carbon-rich end of the curve a decrease of about 40 % is seen. This is accompanied by a dip in the total theoretical curve, primarily due to shorter carbon fibre pull-out lengths and glass fibre debonded lengths.

CONCLUSIONS AND IMPLICATIONS

The use of a model fibrous composite has permitted accurate measurement of fibre debonded length and fibre pull-out length which together with simple models of fracture have enabled a detailed analysis of the mechanisms of cracking in hybrid composites to be undertaken. A negative hybrid effect and a non-linear relationship between work of fracture and fibre composition are due primarily to the effect of the carbon fibres on the post-debond sliding mechanism at the glass fibre/epoxy resin interface. Post-debond friction energy is the dominant term contributing to the fracture energy of glass fibres in epoxy resin, while the fibre debonding energy and fibre pull-out energy terms

are comparable in magnitude. The dominance of the post-debond friction term over the pull-out term for glass fibres is because the debonded lengths are typically 20 times greater than the pull-out lengths. In contrast, the pulling out of broken carbon fibres from a cracked epoxy resin matrix is the principal energy absorbing process for cfrp.

It is important to remember that for structural composites a rule of mixtures relationship between the work of fracture of the hybrids and the cfrp and gfrp composites may overestimate the fracture energy of the hybrid composites.

Acknowledgements

The authors would like to thank Mr. L.N. Phillips of the Royal Aircraft Establishment, Farnborough, for providing some of the material and for valuable discussions with Mr. G.H.K. Rae of Carr Reinforcements, Liverpool, for his help and advice. The continuing assistance of the U.S. Army, contract numner DA-ERO-75-G-009, is appreciated. One of us (MM) is grateful to the National Research Council of Canada for its support in the form of a Post-doctoral Fellowship.

REFERENCES

1. P.W.R. BEAUMONT, J. Adhesion, 6 (1974) 107.

2. P.W.R. BEAUMONT and B. HARRIS, J. Mater. Sci., 7 (1972) 1265.

3. J.O. OUTWATER and M.C. MURPHY, 24th Annual Technical Conference on Reinforced Plastics/Composites Division, Paper 11C (1969), Society of Plastics Industry, Inc.

4. B. HARRIS, J. MORLEY and D.C. PHILLIPS, J. Mater. Sci., 10 (1975) 2050.

5. B. GERSHON and G. MAROM, J. Mater. Sci., 10 (1975) 1549.

6. C.C. CHAMIS, M.P. HANSON and T.T. SERAFINI, ASTM STP 497 (1972) 324.

7. B. HARRIS and A.R. BUNSELL, Composites, 6 (1975) 197.

8. P.W.R. BEAUMONT, P.S. RIEWALD and C. ZWEBEN, ASTM STP 568 (1974) 134.

9. P.G. RIEWALD and C. ZWEBEN, 30th Annual Technical Conference on Reinforced Plastics/Composites Division (1975), Society of Plastics Industry, Inc.

10. P.K. MALLICK and L.J. BROUTMAN, ibid.

11. D.F. ADAMS and A.K. MILLER, Mater. Sci. and Eng., 19 (1975) 245.

12. J.L. PERRY and D.F. ADAMS, Composites, 6 (1975) 166.

13. G.A. COOPER, J. Mater. Sci., 12 (1977) 277.

14. B. HARRIS, P.W.R. BEAUMONT and E. MONCUNILL de FERRAN, J. Mater. Sci., 10 (1971) 238.

15. A.H. COTTRELL, Proc. Roy. Soc. (Lond.) A282 (1964) 2.

PERSONNEL

Dr. Peter W.R. Beaumont is principal investigator.

Dr. John N. Kirk is a post-doctoral research fellow.

Dr. Michael Munro is a post-doctoral research fellow.

Table I. Fibre and Matrix Properties

Material	No. of fibres per tow	Fibre diameter ($\times 10^{-6}$m)	Tensile strength GNm^{-2}	Young's modulus GNm^{-2}	Calculated failure strain ε
Carbon fibre Type II	5000	8	2.40	240	0.010
Glass fibre Type E	1600	13	1.65	70	0.023
Epoxy resin CY219 + HY219	-	-	0.06	2.5	0.024

Table II. Experimental Results

Carbon Fibre Volume Fraction	No. of Specimens	Tape Glass fibre tows / Carbon fibre tows	Predicted rule of mixtures fracture energy (kJm^{-2})	Normalised work of fracture energy (kJm^{-2})	% Difference	GLASS FIBRE		CARBON FIBRE	
						Average debonded length, y ($\times 10^{-3}$ m)	Average maximum pull-out length, $\bar{\ell}_{max}$ ($\times 10^{-3}$m)	Average maximum pull-out length, $\bar{\ell}_{max}$ ($\times 10^{-3}$m)	Average debonded length ($\times 10^{-3}$m)
0.00	5	1:0	-	316 ± 45*	-	5.26	0.46	-	
0.13	4	4:1	288	236 ± 38	-18.1	4.44	0.50	0.64	
0.23	4 3	4:1 3:1	267	197 ± 45	-26.2	4.42	0.44	0.56	
0.37	3 1 2	4:1 3:1 1:1	236	205 ± 32	-13.1	4.70	0.46	0.64	< 1
0.44	7	3:1	221	208 ± 19	-5.9	5.90	0.54	0.66	
0.54	5	1:1	200	171 ± 22	-14.5	5.28	0.52	0.68	
0.64	6	1:1	178	156 ± 26	-12.4	4.26	0.54	0.62	
0.70	6	1:1	165	125 ± 20	-24.2	4.63	0.56	0.56	
0.83	4	1:4	137	83 ± 8	-39.2	2.34	0.38	0.45	
1.00	5	0:1	-	100 ± 19	-	-	-	0.56	

*Mean ± standard deviation

Table III. Theoretical Models of Energy Absorption Fracture Mechanisms

MODEL	EQUATION	REFERENCE
Debonding energy	$\gamma_d = \frac{V_f \sigma_f^2 y}{4E}$	[3]
Post debond friction energy	$\gamma_{pdf} = \frac{V_f \tau y^2 \Delta\varepsilon}{d}$	[4]
Pull-out energy	$\gamma_p = \frac{V_f \sigma_f \ell_c}{24}$	[15]

V_f = volume fractions of carbon or glass fibres in total fibre

σ_f = ultimate tensile strength of carbon or glass fibres

ℓ_c = critical transfer length of fibre

E = Young's modulus of fibre

y = average debonded length of fibre

$\Delta\varepsilon$ = differential failure strain between fibre and matrix

τ = interfacial frictional shear stress

d = fibre diameter

Table IV. Theoretical Fracture Energies

Carbon fibre volume fraction	Glass fibre debond energy γ_d^g (k Jm^{-2})	Glass fibre post debond friction energy γ_{pdf}^g (k Jm^{-2})	Glass fibre pull-out energy γ_p^g (k Jm^{-2})	Carbon fibre pull-out energy γ_p^c (k Jm^{-2})	γ_{TOTAL} (k Jm^{-2})
0.00	51.0 ± 2.0*	257.5 ± 42.2	63.3 ± 9.2	-	371.8 ± 35.2
0.13	37.5 ± 1.9	148.6 ± 27.7	58.9 ± 8.9	16.8 ± 1.4	261.8 ± 21.6
0.23	33.0 ± 2.9	146.9 ± 41.8	47.5 ± 9.0	25.5 ± 4.9	252.9 ± 36.3
0.37	29.1 ± 4.2	136.2 ± 46.0	39.3 ± 6.0	47.7 ± 9.8	252.3 ± 57.2
0.44	32.0 ± 4.0	151.0 ± 49.6	42.1 ± 5.9	57.8 ± 11.1	282.9 ± 67.2
0.54	23.4 ± 1.8	105.8 ± 30.9	32.9 ± 5.7	72.8 ± 6.1	234.9 ± 27.5
0.64	14.7 ± 1.8	50.4 ± 13.6	26.9 ± 2.1	78.4 ± 5.7	170.4 ± 16.5
0.70	11.1 ± 2.1	49.0 ± 75.1	23.4 ± 6.6	76.9 ± 8.6	160.4 ± 47.2
0.83	3.9 ± 0.1	10.5 ± 1.9	8.9 ± 1.3	75.5 ± 5.7	98.8 ± 5.9
1.00	-	-	-	110.4 ± 14.2	110.4 ± 14.2

*Mean ± standard deviation

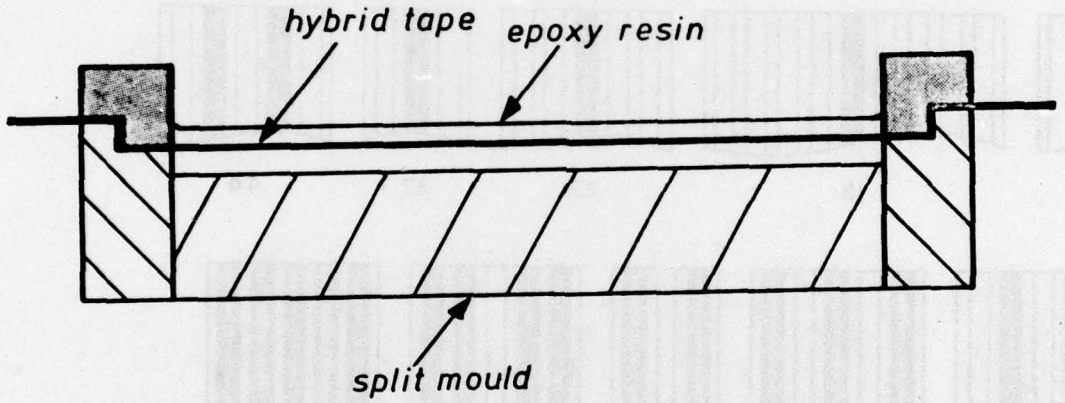

Figure 1 Cross-section of the split frame mould.

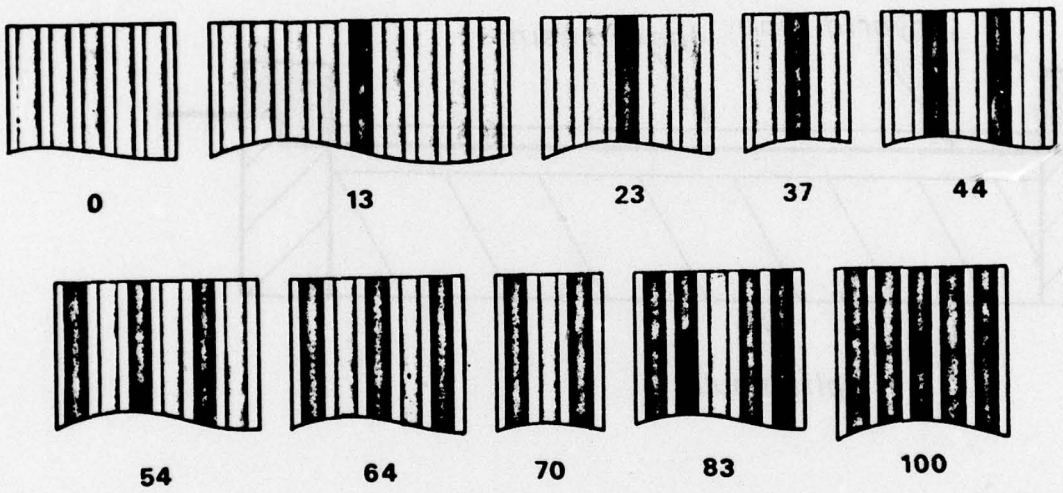

Figure 2 Arrangement of glass fibre tows (grey) and carbon fibre tows (black) for each specimen group. The numbers beneath each diagram give the percentage (by volume) of carbon fibre in total fibre.

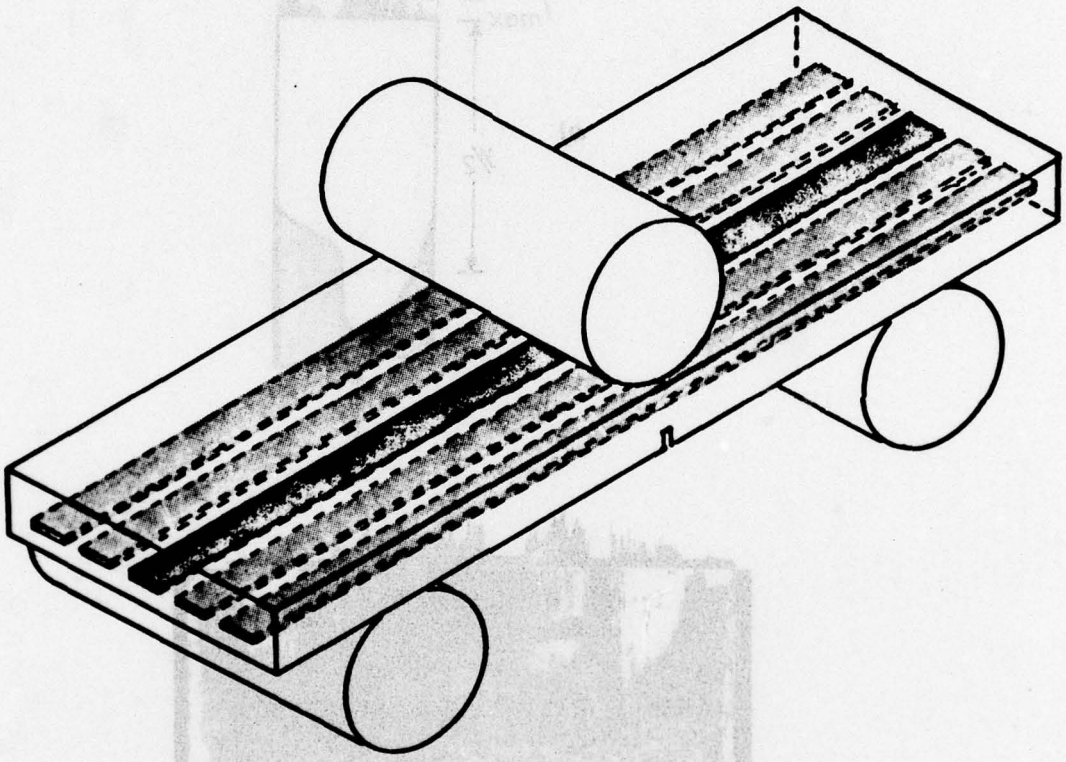

Figure 3 Three point bending beam specimen.

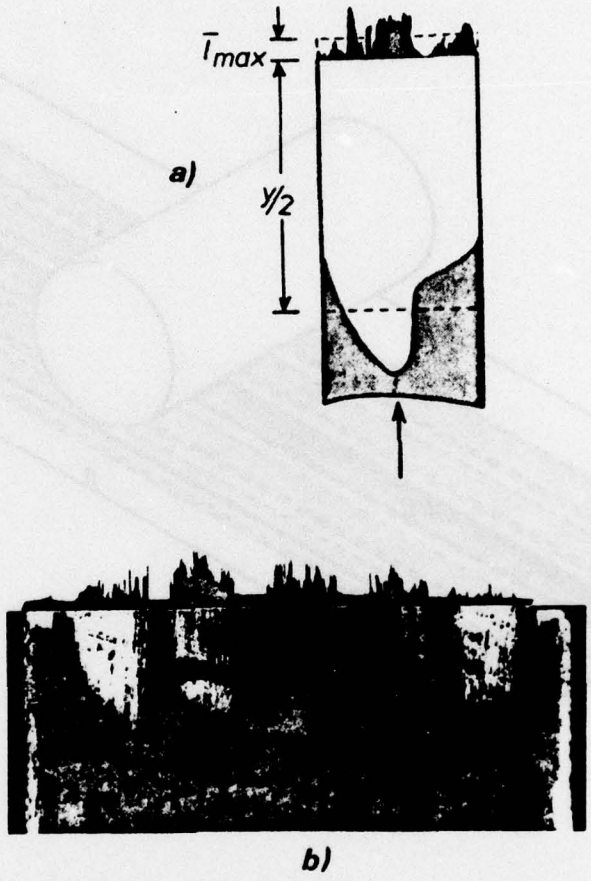

Figure 4 Measurement of the average fibre debonded and pull-out lengths
(a) tracing of the fibre pull-out and debonded regions for a typical tow in (b),
(b) composite photograph of pull-out and debonded regions viewed in transmitted and reflected light respectively. (23 % carbon fibre hybrid specimen).

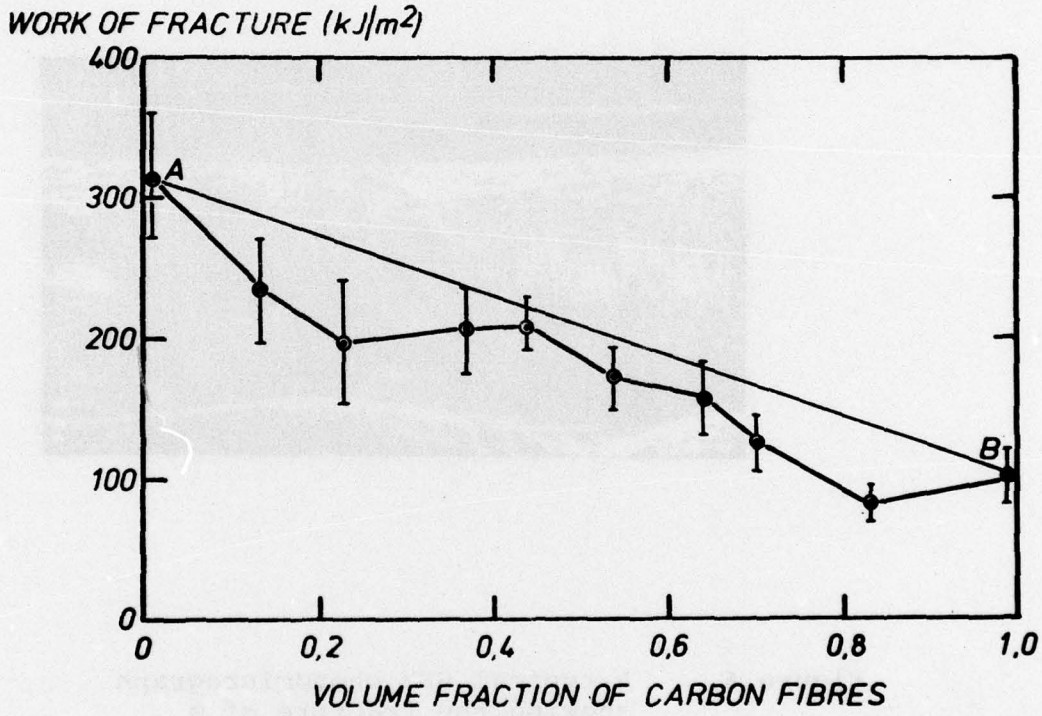

Figure 5 Work of fracture as a function of carbon fibre volume fraction. AB is the rule of mixtures relationship.

Figure 6. A typical SEM photomicrograph showing the fracture of a carbon fibre t (left) and a glass fibre tow. (The marker length is equivalent to 1 mm.)

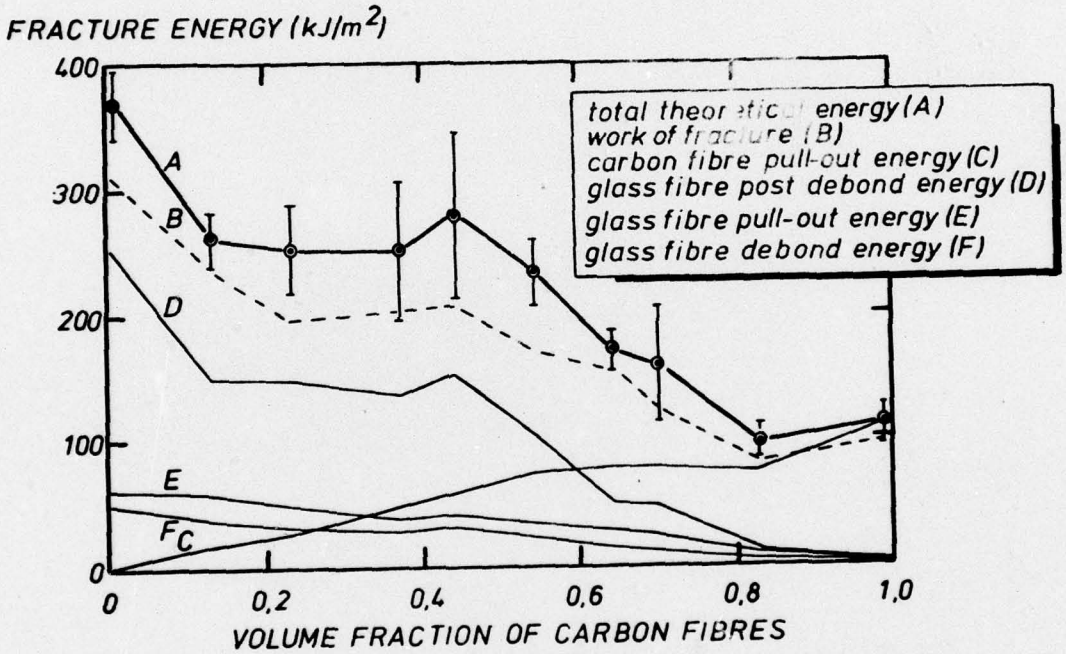

Figure 7 The individual and total theoretical energy terms as a function of carbon fibre volume fraction for the hybrid composite.